

Provided for non-commercial research and education use.
Not for reproduction, distribution or commercial use.

Volume 96, Issue 6, November 2010
Last Issue of this Volume

ISSN 0090-640X

**Atomic Data
AND
Nuclear Data Tables**

A Journal Devoted to Compilations of
Experimental and Theoretical Results

EDITOR:
David R. Schultz

IN MEMORIAM:
S. Raman, Editor

ASSOCIATE EDITORS:
S. M. Austin
John W. Cooper
Bernd Crasemann
A. Dalgarno
J. P. Desclaux
Gordon W. F. Drake
Walter Gibson
Wick C. Haxton
Hideotugu Ikegami
Joachim Jänecke
Kartheinz Langanke
E. Merzbacher
Wilfried Scholz
Stephen M. Shafroth
Pertti Tikkainen
P. J. Twin

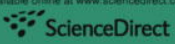
EDITOR EMERITA:
Angela Li-Scholz

FOUNDING EDITOR:
Katherine Way

CONTENTS:

Incident photon energy and Z dependence of L -X-ray relative intensities <i>Anil Kumar, Yogeshwar Chauhan, Sanjiv Puri</i>	567
A critical compilation of experimental data on spectral lines and energy levels of hydrogen, deuterium, and tritium <i>A.E. Kramida</i>	586
Calculations of Maxwellian-averaged cross sections and astrophysical reaction rates using the ENDF/B-VII.0, JEFF-3.1, JENDL-3.3, and ENDF/B-VI.8 evaluated nuclear reaction data libraries <i>B. Pritschek, S.F. Maghaghah, A.A. Sonzogni</i>	645
Discovery of the barium isotopes <i>A. Shore, A. Fritzsch, J.Q. Ginepro, M. Heim, A. Schuh, M. Thoennessen</i>	749
New atomic data for Ti X <i>Jagjit Singh, A.K.S. Jha, N. Verma, M. Mohan</i>	759
Discovery of the iron isotopes <i>A. Schuh, A. Fritzsch, M. Heim, A. Shore, M. Thoennessen</i>	817
Radiative capture of nucleons at astrophysical energies with single-particle states <i>J.T. Huang, C.A. Bertulani, V. Guimaraes</i>	824
Discovery of the cobalt isotopes <i>T. Szymanski, M. Thoennessen</i>	848
Discovery of the cadmium isotopes <i>S. Amos, M. Thoennessen</i>	855
Oscillator strengths and transition probabilities of O II <i>Suman N. Nahar</i>	863
Cumulated Author Index	878
Cumulated Subject Index	897

Available online at www.sciencedirect.com

 ScienceDirect

This article appeared in a journal published by Elsevier. The attached copy is furnished to the author for internal non-commercial research and education use, including for instruction at the authors institution and sharing with colleagues.

Other uses, including reproduction and distribution, or selling or licensing copies, or posting to personal, institutional or third party websites are prohibited.

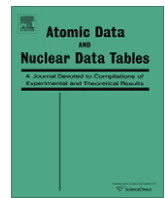
In most cases authors are permitted to post their version of the article (e.g. in Word or Tex form) to their personal website or institutional repository. Authors requiring further information regarding Elsevier's archiving and manuscript policies are encouraged to visit:

<http://www.elsevier.com/copyright>



Contents lists available at ScienceDirect

Atomic Data and Nuclear Data Tables

journal homepage: www.elsevier.com/locate/adt

Oscillator strengths and transition probabilities of O II

Sultana N. Nahar*

Department of Astronomy, The Ohio State University, Columbus, OH 43210, USA

ARTICLE INFO

Article history:

Available online 21 August 2010

ABSTRACT

The abundance of singly ionized oxygen, O II, in planetary nebulae provides crucial diagnostic tests for the physical conditions present in these astrophysical environments. The abundance can be determined from the absorption lines formed by the radiative processes, such as the photo-excitations reported here. Radiative transitions are obtained from a total of 708 fine structure levels of O II with $n \leq 10$, $l \leq 9$, and $1/2 \leq J \leq 17/2$. For spectral analysis oscillator strengths, line strengths, and transition probabilities (A) are presented for 51,733 electric dipole fine structure radiative transitions. The calculations were carried out in the relativistic Breit–Pauli R-matrix approximation. The transitions have been identified spectroscopically using quantum defect analysis and other criteria. The calculated energies agree with the observed energies within 5% for most of the levels. However, some relatively large differences are noted, the largest difference being 13% for the level $2s^2 2p^2 (^1D) 4p (^2F)_{7/2}$. Most of the A values and lifetimes agree with the existing measured and calculated values. The transitions should be applicable for diagnostics as well as spectral modeling in the ultraviolet and optical regions of astrophysical and laboratory plasmas.

© 2010 Elsevier Inc. All rights reserved.

* Fax: +1 517 353 5967.
E-mail address: nahar@astronomy.ohio-state.edu

Contents

1. Introduction	864
2. Theory	864
3. Calculations	865
4. Results and discussion	865
4.1. Fine structure energies	865
4.2. Allowed E1 transitions	866
4.3. Lifetimes	867
5. Conclusions	869
Acknowledgments	869
Appendix A. Supplementary data	869
References	869
Explanation of Tables	870
Tables	
1. Partial set of 708 energy levels of O II, grouped as fine structure components of the LS terms.	871
2. E1 transition probabilities for observed levels of O II, grouped as fine structure components of LS multiplets.	874

1. Introduction

Knowledge of accurate atomic transitions in O II is crucial for predicting its abundances in nebular plasmas and in modeling of supernova remnants and OB type hot stars. Traces of O II are also found in the solar wind. Its diagnostic role in these environment stems from the fact that spectral properties provide information on population. However, a well known, large discrepancy exists in the predicted abundance of the ion depending on the varying considerations of radiative or collisional processes. These processes for O II have been studied by many researchers and, in a previous study, we computed collision strengths of O II [1,2] using the Breit–Pauli R-matrix (BPRM) method. Later Tayal [3] presented similar results considering a larger number of collisional excitations. He also presented the radiative transitions among those levels obtained from atomic structure calculations.

Quite a number of studies have been carried out for radiative transitions and lifetimes of O II, both theoretically, for example, by Lennon and Burke [4] as part of the Opacity Project [5], Bell et al. [6] whose values were renormalized for a number of transitions by Wiese et al. [7], Natarajan [8], Bates and Damgaard [9], Froese Fischer [10], and experimentally, for example, by Edlen [11], Eriksson [12], Patterson and Wenaker [13], Veres and Wiese [14], del Val et al. [15], Coetzter et al. [16], and Nandi et al. [17]. An evaluated compilation of O II transitions from earlier investigations was carried out by Wiese et al. [7]. The study of this important ion continues seeking improved results since being near neutral the ion is sensitive to the quality of the representation of the wavefunction. The present work, within the Iron Project [19], reports a large set ($n \leq 10$) of radiative transitions for this ion obtained using the relativistic BPRM for accurate plasma modelings.

2. Theory

Details of the theoretical background can be found in the papers from the Opacity Project [5] and the Iron Project (e.g., Ref. [20]). A brief outline of the BPRM method in the close-coupling (CC) approximation (e.g., Ref. [21]) is given below. In the CC approximation the atomic system is described as an N -electron target (core) interacting with a $(N+1)$ th electron. The total wavefunction expansion, Ψ_E , of the $(N+1)$ -electron system is written as

$$\Psi_E(e + ion) = A \sum_i \chi_i(iion) \theta_i + \sum_j c_j \Phi_j(e + ion), \quad (1)$$

where χ_i is the target/core ion wavefunction of a specific LS state ($S_l L_i \pi_i$) or fine structure level ($J_i \pi_i$) and θ_i is the wavefunction of the interacting $(N+1)$ th electron in a channel labeled as

$S_l L_i(J_i) \pi_i k_i^2 \ell_i(SL\pi \text{ or } J\pi)$ where k_i^2 is the incident kinetic energy. The sum includes channels of various excitations of the core ion along with wavefunctions of the interacting electron. Φ_j 's are correlation wavefunctions of the $(N+1)$ -electron system that (a) compensate the orthogonality conditions between the continuum and the bound orbitals and (b) represent additional short-range correlation.

In the Breit–Pauli approximation, the relativistic Hamiltonian for the $(N+1)$ -electron system is given by (e.g., Ref. [22])

$$H_{N+1}^{\text{BP}} = H_{N+1} + H_{N+1}^{\text{mass}} + H_{N+1}^{\text{Dar}} + H_{N+1}^{\text{SO}} + \frac{1}{2} \sum_{i \neq j}^N [g_{ij}(so + so') + g_{ij}(ss') + g_{ij}(cs') + g_{ij}(d) + g_{ij}(oo')], \quad (2)$$

where H_{N+1} is the nonrelativistic Hamiltonian,

$$H_{N+1} = \sum_{i=1}^N N + 1 \left\{ -\nabla_i^2 - \frac{2Z}{r_i} + \sum_{j>i}^N N + 1 \frac{2}{r_{ij}} \right\}. \quad (3)$$

H_{N+1}^{mass} is the mass correction, H_{N+1}^{Dar} is the Darwin term, and H_{N+1}^{SO} is the spin-orbit interaction term, respectively. The two-body interaction terms are with notation “ c ” for contraction, “ d ” for Darwin, “ o ” for orbit, “ s ” for spin, and a prime indicates “other”. In the present calculations, the Breit–Pauli R-matrix Hamiltonian within the Iron Project [19] includes the first three one-body corrections and the three two-body terms except the last three weaker terms.

Substitution of the wavefunction expansion into

$$H_{N+1}^{\text{BP}} \Psi_E = E \Psi_E \quad (4)$$

results in a set of coupled equations that are solved using the R-matrix approach. In the BPRM method, the set of $SL\pi$ are recoupled to obtain $(e + ion)$ states with total $J\pi$, following the diagonalization of the $(N+1)$ -electron Hamiltonian. At negative total energies ($E < 0$), the solutions of the close coupling equations occur at discrete eigenvalues of the $(e + ion)$ Hamiltonian that correspond to pure bound states, Ψ_B .

The radiative transition matrix elements with dipole operator, $\mathbf{D} = \sum_i \mathbf{r}_i$, where i is the number of electrons, is given by $\langle \Psi_B | \mathbf{D} | \Psi_{B'} \rangle$ for electric dipole (E1) transitions. These can be reduced to generalized line strengths as

$$S = \left| \left\langle \Psi_f \mid \sum_{j=1}^{N+1} r_j \mid \Psi_i \right\rangle \right|^2 \quad (5)$$

where Ψ_i and Ψ_f are the initial and final bound wavefunctions, respectively. The line strengths are energy independent quantities

and are related to the oscillator strength, f_{ij} , and radiative decay rate or Einstein's A -coefficient (in atomic units, $a.u.$) as

$$f_{ij} = \frac{E_{ji}}{3g_i} S, \quad A_{ji}(a.u.) = \frac{1}{2} \alpha^3 \frac{g_i}{g_j} E_{ji}^2 f_{ij}. \quad (6)$$

E_{ji} is the energy difference between the initial and final states, α is the fine structure constant, and g_i and g_j are the statistical weight factors of the initial and final states, respectively.

The lifetime of a level k can be obtained from the sum of A values of the radiative decays from the level as,

$$\tau_k(s) = \frac{1}{\sum_i A_{ki}(s^{-1})}. \quad (7)$$

In time units, $A_{ji}(s^{-1}) = A_{ji}(a.u.)/\tau_0$, where $\tau_0 = 2.4191 \times 10^{-17}$ s is the atomic unit of time.

3. Calculations

The computations have been carried out using the package of Breit–Pauli R-matrix codes [23,24]. The first step is to obtain the target or core wavefunctions which are the input for “stage 1” (STG1), of the BPRM codes. The wavefunction expansion for the core O III was obtained from optimization of 23 configurations in relativistic atomic structure calculations using the code SUPERSTRUCTURE (SS) [26]. These configurations and the values of Thomas–Fermi–Dirac scaling parameters for the orbitals are listed in Table A. Although all 23 configurations were treated spectroscopically, only the first 19 levels of O III were included in the wavefunction for O II since no more bound states of O II are expected to form beyond these 19 core levels. These levels and comparison of their calculated energies with those of experiment (compiled by NIST [25]) are given in Table A. The observed and calculated energies show good agreement.

The number of partial waves considered for the outer electron was up to $l \leq 14$ and the R-matrix basis set for the orbitals had 14 terms. Being close to neutral, the ion has considerable correla-

Table A

Levels and energies (E_r) of the target (core ion) O III in a wavefunction expansion of O II. They were optimized using a set of 23 spectroscopic configurations: $2s^2 2p^2(1)$, $2s^2 2p^2(2)$, $2s^2 2p^3(3)$, $2p^4(4)$, $2s^2 2p^3(5)$, $2s^2 2p^2 3d(6)$, $2s^2 2p^4(7)$, $2s^2 2p^4(8)$, $2s^2 2p^2 3s(9)$, $2s^2 2p^2 3p(10)$, $2s^2 2p^2 3d(11)$, $2s^2 3s^2(12)$, $2s^2 3p^2(13)$, $2s^2 3d^2(14)$, $2s^2 4s^2(15)$, $2s^2 4p^2(16)$, $2s^2 3s 3p(17)$, $2s^2 3s 3d(18)$, $2s^2 3s 4s(19)$, $2s^2 3p 3d(20)$, $2p^3 3s(21)$, $2p^3 3p(22)$, and $2p^3 3d(23)$ with filled 1s orbital. The Thomas–Fermi scaling parameters for the orbitals are 1.46012(1s), 1.30294(2s), 1.19650(2p), 1.4025(3s), 1.3826(3p), 1.0(3d), 1.0(4s), and 1.0(4p). The present calculated energies (SS) are compared with the observed energies in the NIST compilation [25].

Level	J_t	$E_r(\text{Ry}) \text{ NIST}$	$E_r(\text{Ry}) \text{ SS}$
1	$1s^2 2s^2 2p^2(^3P)$	0	0.0
2	$1s^2 2s^2 2p^2(^3P)$	1	0.0010334
3	$1s^2 2s^2 2p^2(^3P)$	2	0.0027958
4	$1s^2 2s^2 2p^2(^1D)$	2	0.18472
5	$1s^2 2s^2 2p^2(^1S)$	2	0.39352
6	$1s^2 2s 2p^3(^5S^0)$	2	0.54972
7	$1s^2 2s 2p^3(^3D^0)$	3	1.0938
8	$1s^2 2s 2p^3(^3D^0)$	2	1.0940
9	$1s^2 2s 2p^3(^3D^0)$	1	1.0941
10	$1s^2 2s 2p^3(^3P^0)$	2	1.2975
11	$1s^2 2s 2p^3(^3P^0)$	1	1.2975
12	$1s^2 2s 2p^3(^3P^0)$	0	1.2976
13	$1s^2 2s 2p^3(^1D^0)$	2	1.7045
14	$1s^2 2s 2p^3(^5S^0)$	1	1.7960
15	$1s^2 2s 2p^3(^3P^0)$	1	1.9178
16	$1s^2 2s 2p 3s(^3P^0)$	0	2.4354
17	$1s^2 2s 2p 3s(^3P^0)$	1	2.4365
18	$1s^2 2s 2p 3s(^3P^0)$	2	2.4388
19	$1s^2 2s 2p 3s(^3P^0)$	1	2.4885

tion. Hence a relatively large R-matrix sphere, $15a_o$ where a_o is Bohr radius, was chosen for convergence of the orbital wavefunctions. The second term of the wavefunction included 73 configurations of O II with minimum and maximum occupancies, specified within parentheses, $1s(2-2)$, $2s(0-2)$, $2p(0-5)$, $3s(0-2)$, $3p(0-2)$, $3d(0-2)$, $4s(0-2)$, and $4p(0-2)$. In the Hamiltonian matrix, the calculated energies of the O III levels were replaced by the observed values.

The fine structure energy levels of O II were calculated in STGB and the energies were sorted by scanning through the poles in the $(e + ion)$ Hamiltonian with a fine mesh of effective quantum number Δv of 0.001 to 0.0001. The energies were identified through a theoretical spectroscopy procedure based on quantum defect analysis, percentage of channel contributions, and angular momenta algebra as described in Ref. [27] and using code PRCBPID. The oscillator strengths for bound–bound transitions were obtained using code STGBB. The transitions were processed for energies and transition wavelengths using code PBPRAD.

4. Results and discussion

Results are presented here for the fine structure energy levels, oscillator strengths, line strengths, and radiative decay rates for a large number of allowed E1 transitions in O II. The energies and radiative transitions are discussed in the following subsections.

4.1. Fine structure energies

A set of 708 fine structure bound levels of O II, with $n \leq 10$, $0 \leq l \leq 9$, and $1/2 \leq J \leq 17/2$ of even and odd parities are presented. These levels have been identified spectroscopically as $C_t(S_t L_t \pi_t)_J, n l J(SL)\pi$, where $C_t, S_t L_t \pi_t, J_t$ are the configuration, LS term, parity, and total angular momentum of the target or the core, $n l$ are the principal and orbital quantum numbers of the outer or the valence electron, and J and $SL\pi$ are the total angular momentum, LS term, and parity of the $(N+1)$ -electron system.

Spectroscopic identification of the calculated energies is a major effort since the computational procedure of the Breit–Pauli R-matrix method does not identify them. The method of spectroscopic identification with BPRM is different from that of atomic structure calculations. An atomic structure calculation assigns a spectroscopic designation based on the mixing coefficients of the contributing configurations. On the contrary, with a larger number of configurations and couplings of channels involved in BPRM, several considerations such as quantum defects, percentage of channel contributions, and angular momentum algebra need to be made [27]. Hund's rule is followed for levels arising from the same configuration such that the level with higher spin multiplicity ($2S+1$) and higher orbital angular momentum, L , lies lower than that with lower spin multiplicity and angular momentum.

A partial set of identified calculated energy levels is presented in Table 1 where the levels are grouped as LSJ components of LS terms. This form is useful for spectroscopic diagnostics and to check whether a set of levels is complete. The identification program PRCBPID [27] checks the completeness of the set of energy levels that belong to the LS term(s), and states if the set is complete, otherwise lists the missing levels.

Table B presents fine structure level energies in sets of $J\pi$ format. However, in this table the calculated energies have been replaced by the available observed energies. The reason for including the observed energies is improved accuracy in applications. This format is also convenient for accurate modeling. The complete set of 708 energy levels of O II is available electronically.

Although Hund's rule is adopted for identification, it is used more strictly for $(2S+1)$ than for L . It may be noted that some

Table B

Partial set of fine structure energy levels of O II in $J\pi$ order. I_j is the energy index of the level in its symmetry. The last column is the encoded identification of the level.

i_e	$J\pi$	I_j	$E(\text{Ry})$	Config.	$^{2S+1}L^\pi$	$jjppiiii$
1	0.5 e	1	-1.48710E+00	2s2p4	$^4P^e$	100001
2	0.5 e	2	-8.93370E-01	2s22p2(3P)3s	$^4P^e$	100002
3	0.5 e	3	-8.60080E-01	2s22p2(3P)3s	$^2P^e$	100003
4	0.5 e	4	-7.97910E-01	2s2p4	$^2S^e$	100004
5	0.5 e	5	-6.42520E-01	2s2p4	$^2P^e$	100005
6	0.5 e	6	-4.79890E-01	2s22p2(1S)3s	$^2S^e$	100006
7	0.5 e	7	-4.61720E-01	2s22p2(3P)3d	$^4P^e$	100007
8	0.5 e	8	-4.60730E-01	2s22p2(3P)3d	$^4D^e$	100008
9	0.5 e	9	-4.53140E-01	2s22p2(3P)3d	$^2P^e$	100009
10	0.5 e	10	-4.06820E-01	2s22p2(3P)4s	$^4P^e$	100010
11	0.5 e	11	-3.91310E-01	2s22p2(3P)4s	$^2P^e$	100011
12	0.5 e	12	-2.68650E-01	2s22p2(1D)3d	$^2P^e$	100012
13	0.5 e	13	-2.59020E-01	2s22p2(3P)4d	$^4D^e$	100013
14	0.5 e	14	-2.56140E-01	2s22p2(3P)4d	$^4P^e$	100014
15	0.5 e	15	-2.55050E-01	2s22p2(3P)4d	$^2P^e$	100015
16	0.5 e	16	-2.51950E-01	2s22p2(1D)3d	$^2S^e$	100016
17	0.5 e	17	-2.33060E-01	2s22p2(3P)5s	$^4P^e$	100017
18	0.5 e	18	-2.26540E-01	2s22p2(3P)5s	$^2P^e$	100018
19	0.5 e	19	-1.62894E-01	2s22p23P5d	$^4PD^e$	100019
20	0.5 e	20	-1.60441E-01	2s22p23P5d	$^4PD^e$	100020
21	0.5 e	21	-1.60008E-01	2s22p23P5d	$^2P^e$	100021
22	0.5 e	22	-1.51020E-01	2s22p2(3P)6s	$^4P^e$	100022
23	0.5 e	23	-1.47350E-01	2s22p2(3P)6s	$^2P^e$	100023
24	0.5 e	24	-1.13326E-01	2s22p23P6d	$^4PD^e$	100024
25	0.5 e	25	-1.12257E-01	2s22p23P6d	$^4PD^e$	100025
26	0.5 e	26	-1.10294E-01	2s22p23P6d	$^2P^e$	100026
27	0.5 e	27	-1.06570E-01	2s22p23P7s	$^4P^e$	100027
28	0.5 e	28	-1.02763E-01	2s22p23P7s	$^2P^e$	100028
29	0.5 e	29	-1.01934E-01	2s2p3S ¹ 3p	$^4P^e$	100029
30	0.5 e	30	-8.21840E-02	2s22p23P7d	$^4PD^e$	100030
31	0.5 e	31	-8.02704E-02	2s22p23P7d	$^4PD^e$	100031
32	0.5 e	32	-7.96340E-02	2s22p23P7d	$^2P^e$	100032
33	0.5 e	33	-7.74644E-02	2s22p23P8s	$^4P^e$	100033
34	0.5 e	34	-7.58932E-02	2s22p23P8s	$^2P^e$	100034
35	0.5 e	35	-6.62890E-02	2s22p2(1D)4d	$^2S^e$	100035

energies have been designated by more than one L value. These are all calculated levels for which there exists more than one possible value of the total angular momentum, L . For example, in **Table B** the level ($2s^22p^23P5d$) with $J = 1/2$, can have total angular momentum equal to P or D . If Hund's rule is followed, L should be D for the lower level and P for the upper level. However, for a multi-electron system, Hund's rule may not necessarily be followed. For such levels, both values of L are specified in the identification. Hence, for this particular level, the assigned designation is $^4PD_{1/2}$ meaning L could be P or D .

The BPRM energies for O II are compared with the observed values in **Table C**. They agree with those in the NIST compiled table [25] within 5% for most of the levels. However, some relatively large differences are also found, the largest difference being 13% for the level $2s^22p^2(^1D)4p(^2F)_{7/2}$. It may be noted that all levels have been identified uniquely based on the criteria above and with correspondence between the fine structure levels and their LS terms, such that exact numbers of fine structure levels are accounted for each LS term. However, due to mixing of states and similar quantum defects, spectroscopic designations could be swapped with respect to the atomic structure calculations. Hence, each level is assigned with one or more possible designations.

4.2. Allowed E1 transitions

The f , S , and A values for electric dipole transitions (same spin-multiplicities and intercombination) in O II using the *ab initio*

Table C

Comparison of calculated BPRM energies for O II with observed values [25]. I_j is the calculated level index for its position in its $J\pi$ symmetry.

Level	$J:I_j$	$E(\text{Ry}, \text{NIST})$	$E(\text{Ry}, \text{BPRM})$
2s22p3	$^4S^0$	1.5:1	2.58140
2s22p3	$^2D^0$	2.5:1	2.33700
2s22p3	$^2D^0$	1.5:2	2.33690
2s22p3	$^2P^0$	1.5:3	2.21260
2s22p3	$^2P^0$	0.5:1	2.21260
2s2p4	$^4P^e$	2.5:1	1.48930
2s2p4	$^4P^e$	1.5:1	1.48780
2s2p4	$^4P^e$	0.5:1	1.48710
2s2p4	$^2D^e$	2.5:2	1.06880
2s2p4	$^2D^e$	1.5:2	1.06870
2s22p2(3P)3s	$^4P^e$	2.5:3	0.89096
2s22p2(3P)3s	$^4P^e$	1.5:3	0.89241
2s22p2(3P)3s	$^4P^e$	0.5:2	0.89337
2s22p2(3P)3s	$^2P^e$	1.5:4	0.85844
2s22p2(3P)3s	$^2P^e$	0.5:3	0.86008
2s2p4	$^2S^e$	0.5:4	0.79791
2s22p2(3P)3p	$^2S^0$	0.5:2	0.72290
2s22p2(3P)3p	$^4D^0$	3.5:1	0.69501
2s22p2(3P)3p	$^4D^0$	2.5:2	0.69614
2s22p2(3P)3p	$^4D^0$	1.5:4	0.69698
2s22p2(3P)3p	$^4D^0$	0.5:3	0.69749
2s22p2(1D)3s	$^2D^e$	2.5:4	0.69529
2s22p2(1D)3s	$^2D^e$	1.5:5	0.69528
2s22p2(3P)3p	$^4P^o$	2.5:3	0.68151
2s22p2(3P)3p	$^4P^o$	1.5:5	0.68234
2s22p2(3P)3p	$^4P^o$	0.5:4	0.68277
2s22p2(3P)3p	$^2D^o$	2.5:4	0.65209
2s22p2(3P)3p	$^2D^o$	1.5:6	0.65382
2s22p2(3P)3p	$^4S^0$	1.5:7	0.64799
2s2p4	$^2P^e$	1.5:6	0.64406
2s2p4	$^2P^e$	0.5:5	0.64252
2s22p2(3P)3p	$^2P^o$	1.5:8	0.62915
2s22p2(3P)3p	$^2P^o$	0.5:5	0.62969
2s22p2(1D)3p	$^2F^0$	3.5:2	0.49685
2s22p2(1D)3p	$^2F^0$	2.5:5	0.49707

close-coupling approximation in the relativistic BPRM method have been obtained for the first time. Previously published results for fine structure transitions were obtained from various atomic structure calculations. One advantage of the R-matrix method is consideration of a large number of transitions. The present set, containing 51,733 E1 transitions among the 708 fine structure levels, is the largest set compared to all existing published sets of transitions.

Table D presents a sample of f , S , and A values contained in the complete file. The top line specifies the nuclear charge ($Z = 8$) and number of electrons in the ion ($N_{elc} = 7$). This line is followed by sets of transitions among various pairs of symmetries, $J_i\pi_i - J_k\pi_k$. The first line of each set specifies the transitional symmetries expressed by their statistical weight factors, $g = 2J + 1$, and parity π (0 for even and 1 for odd parity). The same line also gives the number of levels N_i and N_k belonging to symmetries J_i and J_k , and the total number of transitions $NN = N_i \times N_k$. The transitional levels can be identified spectroscopically by matching their indices I_i and I_k with those in **Table B**. The third column lists the transition wavelengths (λ) in Å obtained using $E(\text{\AA}) = 911.2671/E_{ik}(\text{Ry})$, while the fourth and fifth columns provide individual level energies E_i and E_k in Rydbergs. The sixth column gives the oscillator strength f in length formulation. The sign of f indicates the upper and lower levels in the transition; a negative value means level k is lower. Column seven is line strength S , and column eight is transition probability or the radiative decay rate $A_{ki}(\text{s}^{-1})$. Since f and A values depend on the transition energies, they have been evaluated from the

Table DSample of f , S , and A values for allowed E1 transitions in O II (see text in Results and Discussions section for explanation of the table).

I_i	I_k	$\lambda(\text{\AA})$	$E_i(\text{Ry})$	$E_k(\text{Ry})$	f	S	$A_{ki}(\text{s}^{-1})$
							2 0 2 1 47 43 2021 = gi Pi gk Pk Ni Nk NN (= Ni times Nk)
1	1	1256.05	-1.4871E+00	-2.2126E+00	2.532E-07	2.094E-06	1.071E+03
1	2	1192.45	-1.4871E+00	-7.2290E-01	-7.265E-07	5.704E-06	3.407E+03
1	3	1154.07	-1.4871E+00	-6.9749E-01	-1.101E-03	8.368E-03	5.514E+06
1	4	1132.95	-1.4871E+00	-6.8277E-01	-1.578E-03	1.177E-02	8.202E+06
1	5	1062.81	-1.4871E+00	-6.2969E-01	-4.746E-08	3.321E-07	2.802E+02
1	6	889.68	-1.4871E+00	-4.6284E-01	-2.105E-09	1.233E-08	1.774E+01
1	7	800.28	-1.4871E+00	-3.4841E-01	-9.751E-07	5.138E-06	1.016E+04
1	8	795.62	-1.4871E+00	-3.4175E-01	-1.513E-05	7.924E-05	1.594E+05
1	9	792.14	-1.4871E+00	-3.3672E-01	-2.555E-04	1.332E-03	2.715E+06
1	10	779.15	-1.4871E+00	-3.1753E-01	-1.547E-08	7.938E-08	1.700E+02
1	11	752.41	-1.4871E+00	-2.7597E-01	-2.124E-10	1.052E-09	2.502E+00
1	12	735.96	-1.4871E+00	-2.4890E-01	-4.399E-04	2.132E-03	5.417E+06
1	13	711.21	-1.4871E+00	-2.0581E-01	-1.747E-06	8.181E-06	2.304E+04
1	14	710.07	-1.4871E+00	-2.0375E-01	-2.325E-09	1.087E-08	3.076E+01
1	15	708.55	-1.4871E+00	-2.0099E-01	-9.566E-05	4.463E-04	1.272E+06
1	16	703.20	-1.4871E+00	-1.9122E-01	-5.347E-08	2.476E-07	7.213E+02
1	17	685.67	-1.4871E+00	-1.5809E-01	-3.071E-04	1.386E-03	4.356E+06
1	18	678.52	-1.4871E+00	-1.4408E-01	-1.214E-06	5.424E-06	1.758E+04
1	19	674.36	-1.4871E+00	-1.3579E-01	-3.282E-06	1.457E-05	4.812E+04
1	20	672.86	-1.4871E+00	-1.3277E-01	-4.631E-05	2.052E-04	6.822E+05
1	21	672.08	-1.4871E+00	-1.3120E-01	-2.438E-06	1.079E-05	3.601E+04
1	22	665.76	-1.4871E+00	-1.1834E-01	-4.669E-08	2.046E-07	7.025E+02
1	23	661.18	-1.4871E+00	-1.0885E-01	-2.078E-04	9.045E-04	3.170E+06
1	24	655.02	-1.4871E+00	-9.5886E-02	-3.516E-09	1.516E-08	5.465E+01
1	25	654.79	-1.4871E+00	-9.5402E-02	-7.575E-06	3.266E-05	1.178E+05
1	26	654.15	-1.4871E+00	-9.4055E-02	-2.738E-05	1.179E-04	4.268E+05
1	27	652.20	-1.4871E+00	-8.9871E-02	-4.175E-07	1.793E-06	6.546E+03
1	28	647.25	-1.4871E+00	-7.9184E-02	-1.423E-04	6.064E-04	2.265E+06
1	29	643.85	-1.4871E+00	-7.1758E-02	-2.007E-07	8.507E-07	3.229E+03
1	30	643.55	-1.4871E+00	-7.1096E-02	-8.759E-06	3.711E-05	1.411E+05
1	31	643.09	-1.4871E+00	-7.0098E-02	-1.519E-05	6.431E-05	2.450E+05
1	32	641.94	-1.4871E+00	-6.7542E-02	-9.026E-07	3.815E-06	1.461E+04
1	33	640.06	-1.4871E+00	-6.3387E-02	-1.380E-08	5.815E-08	2.247E+02
1	34	638.52	-1.4871E+00	-5.9940E-02	-1.003E-04	4.219E-04	1.642E+06

calculated S values but using the observed transition energies whenever available. The file containing the complete set of transitions as well as the complete set of energies in Table D (for easy correspondence between transitions and identifications) is available electronically.

A set of transitions, 4650 in total, for O II has been reprocessed with complete spectroscopic identification using the observed fine structure levels available in the NIST tabulation. Table 2 presents a partial set of transitions among these observed levels. The transitions have been grouped together as fine structure components of LS multiplets. Fine structure transitions with same spin-multiplicity can be added statistically for f , S , and A values of dipole allowed LS multiplets. The standard spectroscopic notation used in the table can facilitate direct comparison with experiments and other applications, such as diagnostics.

BPRM A values for E1 transitions in O II are compared with those obtained experimentally and theoretically in Table E. Wiese et al. [7] carried out an evaluated compilation of results by various authors which is available at the NIST [25] website. Comparisons of present work for transitions from the ground configuration of O II are made with those by Bell et al. [6] obtained using the CIV3 code, by Tayal [3] obtained from atomic structure calculations using the multi-configuration Hartree-Fock method, by Natarajan [8] obtained using multi-configuration Dirac-Fock approximation, and by Lennon and Burke [4] in the R-matrix method but in nonrelativistic LS coupling approximation. Experimental measurements correspond mainly to $3s - 3p$, $3p - 3d$, and $3d - 4f$ transitions. Wavelengths of the transitions were measured by Edlen [11], Erikson [12], and Pettersson and Wenaker [13]. The present A values agree well with the published results by Tayal [3] and Natarajan [8], and very well with those of Bell et al. [6], some of which

were renormalized later by Wiese et al. [7]. The correlation interaction between $2s2p^4P$ and $2s^22p^23s^4P$ states are known to show considerable perturbation effect on the states. In the latest published results on O II transitions, Tayal [3] accounted for the interaction by introducing a set of correlation orbitals, s, p, d , that were optimized for each state of the configurations. The average radii of the correlation orbitals were close to those of the spectroscopic orbitals indicating the states were very well represented. In contrast the present calculations included optimized orbitals up to $4p$ along with 73 configurations of O II as described in the computation section. These differences are the possible reasons for the differences in A values obtained by Tayal and the present calculations. Good agreement is found between the present values and those listed on the NIST website [25] that it calculated from pure LS coupling. The present A values agree very well with the measured values by Val et al. [15] who used a pulsed discharge lamp, and by Veres and Wiese [14] who used a photoelectric measurement using a well-stabilized arc discharge.

4.3. Lifetimes

Lifetimes of all 707 excited fine structure levels of O II are available electronically, and a sample of lifetimes is given in Table F. They are obtained using the E1 transition probabilities. The last column in the table lists the number of transitions of the level to lower levels.

The present lifetimes are compared with published values in Table G. Lifetimes were measured by Coetzer et al. [16] using the beam-foil technique but applying an arbitrarily normalized decay curve, and by Nandi et al. [17] using the beam-foil technique. The comparison shows that the present lifetimes agree better with

Table E

Comparison of the present A values for E1 transitions in O II with those in Refs. [6,7](a), [3](b), [6](c), [25](d), [8](e), [4](f), [14](g), [15](h). Alphabetic capital letters are the accuracy ratings by NIST.

$\lambda(\text{\AA})$	$A(\text{s}^{-1})$:Theory	Present	Expt.	Transition: $C_i - C_f$	$LS\pi_i - LS\pi_f$	$g_i - g_f$
832.758	8.67e+08 ^a :B+, 9.85e+08 ^b	8.65e+08		2s22p3 – 2s2p4	⁴ S ^o – ⁴ P	4-2
833.330	8.65e+08 ^a :B+, 9.83e+08 ^b	8.62e+08		2s22p3 – 2s2p4	⁴ S ^o – ⁴ P	4-4
834.465	8.61e+08 ^a :B+, 9.78e+08 ^b	8.58e+08		2s22p3 – 2s2p4	⁴ S ^o – ⁴ P	4-6
539.086	9.83e+08 ^a :B+, 8.60e+08 ^b	9.98e+08		2s22p3 – 2s22p2(3P)3s	⁴ S ^o – ⁴ P	4-6
539.854	9.81e+08 ^a :B+, 8.59e+08 ^b	9.96e+08		2s22p3 – 2s22p2(3P)3s	⁴ S ^o – ⁴ P	4-2
539.547	9.81e+08 ^a :B+, 8.59e+08 ^b , 1.04e+09 ^e	9.96e+08		2s22p3 – 2s22p2(3P)3s	⁴ S ^o – ⁴ P	4-4
429.918	4.25e+09 ^a :B+, 4.04e+09 ^b , 3.07e+09 ^e	4.15e+09		2s22p3 – 2s22p2(3P)3d	⁴ S ^o – ⁴ P	4-2
430.176	4.36e+09 ^a :B+, 2.92e+09 ^e	3.35e+09		2s22p3 – 2s22p2(3P)3d	⁴ S ^o – ⁴ P	4-6
430.041	4.13e+09 ^a :B+, 2.95e+09 ^e	3.94e+09		2s22p3 – 2s22p2(3P)3d	⁴ S ^o – ⁴ P	4-4
429.653	6.35e+08 ^c , 1.04e+08 ^c :C	2.80e+08		2s22p3 – 2s22p2(3P)3d	⁴ S ^o – ⁴ D	4-4
429.650	3.49e+08 ^c :C	6.37e+08		2s22p3 – 2s22p2(3P)3d	⁴ S ^o – ⁴ D	4-6
426.522	2.06e+06 ^c :C	3.11e+06		2s22p3 – 2s22p2(3P)3d	⁴ S ^o – ² D	4-6
429.560	6.52e+07 ^c :D	7.64e+07		2s22p3 – 2s22p2(3P)3d	⁴ S ^o – ² F	4-6
418.5958	1.86e+08 ^d :C+	1.89e+08		2s22p3 – 2s22p2(3P)4s	⁴ S ^o – ⁴ P	4-6
418.8786	1.86e+08 ^d :C+	1.85e+08		2s22p3 – 2s22p2(3P)4s	⁴ S ^o – ⁴ P	4-4
419.0633	1.86e+08 ^d :C+	1.83e+08		2s22p3 – 2s22p2(3P)4s	⁴ S ^o – ⁴ P	4-2
391.9062	2.38e+09 ^d :C+	2.28e+09		2s22p3 – 2s22p2(3P)4d	⁴ S ^o – ⁴ P	4-2
391.9380	2.38e+09 ^d :C+	2.14e+09		2s22p3 – 2s22p2(3P)4d	⁴ S ^o – ⁴ P	4-4
391.9954	2.38e+09 ^d :C+	1.80e+09		2s22p3 – 2s22p2(3P)4d	⁴ S ^o – ⁴ P	4-6
388.055	5.58e+07 ^d :C+	6.13e+07		2s22p3 – 2s22p2(3P)5s	⁴ S ^o – ⁴ P	4-2
387.898	5.58e+07 ^d :C+	6.37e+07		2s22p3 – 2s22p2(3P)5s	⁴ S ^o – ⁴ P	4-4
387.649	5.59e+07 ^d :C+	6.76e+07		2s22p3 – 2s22p2(3P)5s	⁴ S ^o – ⁴ P	4-6
1083.139	2.55e+07 ^a :B	2.76e+07		2s2p4 – 2s22p2(3P)3p	⁴ P – ⁴ S ^o	6-4
1085.052	1.82e+07 ^a :B	1.99e+07		2s2p4 – 2s22p2(3P)3p	⁴ P – ⁴ S ^o	4-4
1086.024	9.44e+06 ^a :C+	1.04e+07		2s2p4 – 2s22p2(3P)3p	⁴ P – ⁴ S ^o	2-4
4325.76	1.49e+07 ^c , 1.64e+07 ^f , 1.53e+07 ^e	1.43E+07	1.35e+07 ^g	2s22p2(3P)3s – 2s22p2(3P)3p	⁴ P – ⁴ P ^o	2-2
4317.14	4.32e+07 ^b , 4.12e+07 ^f , 4.03e+07 ^e	3.83e+07	3.40e+07 ^g , 4.11e+07 ^h	2s22p2(3P)3s – 2s22p2(3P)3p	⁴ P – ⁴ P ^o	2-4
4336.86	1.91e+07 ^b , 1.62e+07 ^c , 1.30e+07 ^f , 1.60e+07 ^e	1.62E+07	1.44e+07 ^g , 1.66e+07 ^h	2s22p2(3P)3s – 2s22p2(3P)3p	⁴ P – ⁴ P ^o	4-4
4069.62	1.45e+08 ^c , 1.40e+08 ^f	1.43E+08	1.40e+08 ^g	2s22p2(3P)3p – 2s22p2(3P)3d	⁴ D ^o – ⁴ F	2-4
4078.84	5.35e+07 ^c , 5.59e+07 ^f	5.24E+07	5.07e+07 ^g , 4.44e+07 ^h	2s22p2(3P)3p – 2s22p2(3P)3d	⁴ D ^o – ⁴ F	4-4
4069.88	1.58e+08 ^c , 1.50e+08 ^f , 1.43e+08 ^e	1.53E+08	1.41e+08 ^g	2s22p2(3P)3p – 2s22p2(3P)3d	⁴ D ^o – ⁴ F	4-6
4085.11	4.48e+07 ^c , 4.82e+07 ^f , 5.59e+07 ^e	4.33E+07	4.18e+07 ^g , 4.65e+07 ^h	2s22p2(3P)3p – 2s22p2(3P)3d	⁴ D ^o – ⁴ F	6-6
4094.14	3.37e+06 ^c , 3.93e+06 ^f	3.25E+06	4.32e+06 ^g	2s22p2(3P)3p – 2s22p2(3P)3d	⁴ D ^o – ⁴ F	8-6
4072.15	1.77e+08 ^c , 1.71e+08 ^f , 1.66e+08 ^e	1.74E+08	1.82e+08 ^g , 1.677e+08 ^h	2s22p2(3P)3p – 2s22p2(3P)3d	⁴ D ^o – ⁴ F	6-8
4106.02	1.46e+06 ^c , 1.88e+06 ^f	1.36E+06	1.56e+06 ^g	2s22p2(3P)3p – 2s22p2(3P)3d	⁴ D ^o – ⁴ F	8-6
4092.93	2.46e+07 ^c , 2.80e+07 ^f	2.36E+07	2.44e+07 ^g , 2.28e+07 ^h	2s22p2(3P)3p – 2s22p2(3P)3d	⁴ D ^o – ⁴ F	8-8
4075.86	2.00e+08 ^c , 1.99e+08 ^f	1.98E+08	1.94e+08 ^g , 1.883e+08 ^h	2s22p2(3P)3p – 2s22p2(3P)3d	⁴ D ^o – ⁴ F	8-10

Table F

Sample of lifetimes of O II levels obtained from E1 transitions.

Level	J	I_J	$E(\text{Ry})$	Lifetime (s)	#transitions
1	2s22p2(3P)3s	4Pe	0.5	2 –8.9337E-01	1.003E-09
2	2s22p2(3P)3s	2Pe	0.5	3 –8.6008E-01	2.588E-10
3	2s2p4	2Se	0.5	4 –7.9791E-01	1.894E-10
4	2s2p4	2Pe	0.5	5 –6.4252E-01	1.577E-10
5	2s22p2(1S)3s	2Se	0.5	6 –4.7989E-01	4.280E-09
6	2s22p2(3P)3d	4Pe	0.5	7 –4.6172E-01	2.317E-10
7	2s22p2(3P)3d	4De	0.5	8 –4.6073E-01	9.884E-10
8	2s22p2(3P)3d	2Pe	0.5	9 –4.5314E-01	1.743E-10
9	2s22p2(3P)4s	4Pe	0.5	10 –4.0682E-01	2.223E-09
10	2s22p2(3P)4s	2Pe	0.5	11 –3.9131E-01	7.153E-10
11	2s22p2(1D)3d	2Pe	0.5	12 –2.6865E-01	9.562E-10
12	2s22p2(3P)4d	4De	0.5	13 –2.5902E-01	1.006E-09
13	2s22p2(3P)4d	4Pe	0.5	14 –2.5614E-01	4.321E-10
14	2s22p2(3P)4d	2Pe	0.5	15 –2.5505E-01	5.210E-10
15	2s22p2(1D)3d	2Se	0.5	16 –2.5195E-01	5.249E-10
16	2s22p2(3P)5s	4Pe	0.5	17 –2.3306E-01	4.605E-09
17	2s22p2(3P)5s	2Pe	0.5	18 –2.2654E-01	1.735E-09
18	2s22p2 3Pe 5d	4 PD e	0.5	19 –1.6289E-01	7.822E-09
19	2s22p2 3Pe 5d	4 PD e	0.5	20 –1.6044E-01	7.199E-10
20	2s22p2 3Pe 5d	2 P e	0.5	21 –1.6001E-01	1.102E-09

Table G

Comparison of the present lifetimes τ in ns (10^{-9} s) of O II with those in Refs. [16](a), [17](b), [9](c), [10](d), [18](e), [4](f). NTr represents the number of radiative decays of the level.

Level	τ (ns):Expt.	Present	NTr	Others
$2s22p2(1D)3p$	$^2F_{5/2}^0$	9.67(0.48) ^a	9.06	10 11.5 ^c , 9.86 ^d
$2s22p2(1D)3p$	$^2D_{5/2}^0$	7.40(0.4) ^b	7.03	10 6.0 ^e
$2s22p2(3P)3d$	$^4D_{7/2}^e$	4.14(0.5) ^b	3.931	8 4.16 ^e
$2s22p2(3P)4s$	$^4P_{5/2}^e$	1.9(0.2) ^b	2.207	18 2.24 ^f
$2s22p2(3P)4s$	$^4P_{3/2}^e$	1.9(0.2) ^b	2.210	22 2.24 ^f
$2s22p2(1D)4s$	$^2D_{3/2}^e$	1.2(0.1) ^b	1.464	47 1.3 ^f
$2s22p2(3Pe)4f$	$^2F_{5/2}^0$	3.98(0.48) ^a	3.995	45 3.87 ^c
$2s22p2(3Pe)4f$	$^2G_{9/2}^0$	4.19(0.23) ^a	3.954	11 4.26 ^c
$2s22p2(1De)4f$	$^2F_{5/2}^0$	3.95(0.28) ^a	3.954	139 4.19 ^c

the measured values compared to the values calculated by Bates and Damgaard [9] and Froese Fischer [10].

5. Conclusions

A large set of transition probabilities and oscillator strengths for E1 transitions in O II from the *ab initio* relativistic BPRM method is presented. The atomic data comprises 51,733 transitions among 708 fine structure levels with $n \leq 10$. Comparisons with existing energies, A values, and lifetimes show very good agreement with the measured as well as other theoretical values for most levels and transitions. The fine structure levels are identified spectroscopically. However, due to mixing of levels with different weights and similar quantum defects, the present identifications may not necessarily match those from atomic structure calculations, especially for the high lying levels.

Based on the comparison with various experiments and theoretical work and accuracy of the *ab initio* BPRM method, the present set of transitions is more complete and is of comparable or higher accuracy to existing values, and hence is expected to provide a more accurate basis for astrophysical modeling.

Acknowledgments

This work was partially supported by the NASA APRA program. The computational work was carried out on the Cray X1 at the Ohio Supercomputer Center in Columbus, Ohio.

Appendix A. Supplementary data

Supplementary data associated with this article can be found, in the online version, at doi:10.1016/j.adt.2010.07.002.

References

- [1] M. Montenegro, W. Eissner, S.N. Nahar, A.K. Pradhan, J. Phys. B 39 (2006) 1863.
- [2] K. Pradhan, M. Montenegro, S.N. Nahar, W. Eissner, Mon. Not. R. Astron. Soc. Lett. 366 (2006) L6.
- [3] S. Tayal, Astrophys. J. Suppl. 171 (2007) 331.
- [4] D.J. Lennon, V.M. Burke (unpublished). Data available at the Opacity Database, TOPbase at <<http://cdsweb.u-strasbg.fr/topbase/topbase.html>>.
- [5] The Opacity Project Team, The Opacity Project, vol. 1, 1995, vol. 2, 1996, Institute of Physics Publishing, Bristol, UK.
- [6] K.L. Bell, A. Hibbert, R.P. Stafford, B.M. McLaughlin, Phys. Scr. 50 (1994) 343. some of their values available at NIST were renormalized by Wiese et al. [7].
- [7] W.L. Wiese, J.R. Fuhr, T.M. Deters, J. Phys. Chem. Ref. Data, Monograph No. 7 (1996).
- [8] L. Natarajan, J. Quant. Spectros. Radiat. Transfer 97 (2006) 267.
- [9] D.R. Bates, A. Damgaard, Philos. Trans. R. Soc. Lond. A 242 (1949) 101.
- [10] C. Froese Fischer, Comput. Phys. Commun. 14 (1978) 145.
- [11] B. Edlen, Nova Acta Reg. Soc. Sci. Upsaliensis [IV] 9 (6) (1934).
- [12] K.B.S. Eriksson, J. Opt. Soc. Am. B 4 (1987) 1369.
- [13] S.-G. Patterson, I. Wenaker, Phys. Scr. 42 (1990) 187.
- [14] G. Veres, W.L. Wiese, Phys. Rev. A 54 (1996) 1999.
- [15] J.A. del Val, J.A. Aparicio, V.R. Gonzalez, S. Mar, J. Phys. B 34 (2001) 4531.
- [16] F.J. Coetzer, T.C. Kotze, P. van der Westhuizen, Z. Phys. A 322 (1985) 357.
- [17] T. Nandi, P. Marketos, N. Bhattacharya, S.K. Mitra, J. Phys. B 32 (1999) 769.
- [18] P. Marketos, T. Nandi, Z. Phys. D 42 (1997) 237.
- [19] D.G. Hummer, K.A. Berrington, W. Eissner, A.K. Pradhan, H.E. Saraph, J.A. Tully, Astron. Astrophys. 279 (1993) 298.
- [20] S.N. Nahar, W. Eissner, G.X. Chen, A.K. Pradhan, Astron. Astrophys. 408 (2003) 789.
- [21] M.J. Seaton, J. Phys. B 20 (1987) 6363.
- [22] W. Eissner, in: S. Wilson et al. (Eds.), The Effects of Relativity on Atoms, Molecules, and the Solid State, Plenum Press, New York, 1991, p. 55.
- [23] K.A. Berrington, P.G. Burke, K. Butler, M.J. Seaton, P.J. Storey, K.T. Taylor, Yu Yan, J. Phys. B 20 (1987) 6379.
- [24] K.A. Berrington, W. Eissner, P.H. Norrington, Comput. Phys. Commun. 92 (1995) 290.
- [25] National Institute of Standards and Technology (NIST), Compilation of atomic data are available at <<http://www.nist.gov/physlab/data/asd.cfm>>.
- [26] W. Eissner, M. Jones, H. Nussbaumer, Comput. Phys. Commun. 8 (1974) 270.
- [27] S.N. Nahar, A.K. Pradhan, Phys. Scr. 61 (2000) 675.

Explanation of Tables

Table 1.

Partial set of 708 energy levels of O II, grouped as fine structure components of the *LS* terms. The levels are designated as $C_t(S_tL_t\pi_t)J_tnlj(SL)\pi$. The top line of each set provides the expected number of fine structure levels (Nlv) for the possible $(2S+1)L^\pi$ terms with the given configuration. In the set, the spin multiplicity ($2S+1$) and parity π are fixed, but L varies. Within parentheses next to each L , all possible J values associated with the given *LS* term are specified. This line is followed by the set of energy levels of the same configuration. $Nlv(c)$ at the end specifies the total number of calculated J levels found for the set. If $Nlv = Nlv(c)$, the calculated energy set for the given terms is complete

C_t	target configuration
$S_tL_t\pi_t$	$SL\pi$ symmetry of the target
J_t	total angular momentum of the target state
nl	configuration of the valence electron
J	total angular momentum of the level
$E(\text{Ry})$	energy level in Rydbergs
v	effective quantum number (No v for equivalent electron states; set to 0 for convenience)
$SL\pi$	symmetry of the level

Table 2.

E1 transition probabilities for observed levels of O II, grouped as fine structure components of *LS* multiplets

$C_{i,k}$	configurations of transitional levels
T_i	<i>LS</i> term designation of the level
g_i	statistical weight factor ($2J+1$) of the level
I	position index of the level in its $SL\pi$ symmetry
E_{ik}	transition energy
f, S, A	oscillator strength, line strength, radiative decay rate

Table 1Partial set of 708 energy levels of O II, grouped as fine structure components of the LS terms. See page 870 for Explanation of Tables.

$C_t(S_t L_t \pi_t)$	J_t	nl	$2J$	$E(\text{Ry})$	v	$SL\pi$
Eqv electron/unidentified levels, parity: o						
2s22p3			3	-2.58813E+00	0.00	4S o
Nlv(c) = 1: set complete						
Eqv electron/unidentified levels, parity: o						
2s22p3			3	-2.32644E+00	0.00	2D o
2s22p3			5	-2.32636E+00	0.00	2D o
Nlv(c) = 2: set complete						
Eqv electron/unidentified levels, parity: o						
2s22p3			1	-2.18985E+00	0.00	2P o
2s22p3			3	-2.18983E+00	0.00	2P o
Nlv(c) = 2: set complete						
Eqv electron/unidentified levels, parity: e						
2s2p4			5	-1.47632E+00	0.00	4P e
2s2p4			3	-1.47506E+00	0.00	4P e
2s2p4			1	-1.47432E+00	0.00	4P e
Nlv(c) = 3: set complete						
Eqv electron/unidentified levels, parity: e						
2s2p4			3	-1.02566E+00	0.00	2D e
2s2p4			5	-1.02560E+00	0.00	2D e
Nlv(c) = 2: set complete						
Nlv = 3, $^4L^e$: P (5 3 1)/2						
2s22p2 (3Pe)	0	3s	1	-8.87824E-01	2.12	4P e
2s22p2 (3Pe)	1	3s	3	-8.86848E-01	2.12	4P e
2s22p2 (3Pe)	1	3s	5	-8.85216E-01	2.12	4P e
Nlv(c) = 3: set complete						
Nlv = 2, $^2L^e$: P (3 1)/2						
2s22p2 (3Pe)	1	3s	1	-8.54004E-01	2.16	2P e
2s22p2 (3Pe)	1	3s	3	-8.52172E-01	2.16	2P e
Nlv(c) = 2: set complete						
Eqv electron/unidentified levels, parity: e						
2s2p4			1	-7.38436E-01	0.00	2S e
Nlv(c) = 1: set complete						
Nlv = 5, $^2L^o$: S (1)/2 P (3 1)/2 D (5 3)/2						
2s22p2 (3Pe)	0	3p	1	-7.17960E-01	2.36	2SP o
2s22p2 (3Pe)	1	3p	3	-6.44892E-01	2.49	2PD o
2s22p2 (3Pe)	1	3p	5	-6.42900E-01	2.49	2D o
2s22p2 (3Pe)	1	3p	1	-6.19412E-01	2.54	2SP o
2s22p2 (3Pe)	2	3p	3	-6.18676E-01	2.54	2PD o
Nlv(c) = 5: set complete						
Nlv = 8, $^4L^o$: S (3)/2 P (5 3 1)/2 D (7 5 3 1)/2						
2s22p2 (3Pe)	0	3p	1	-6.92048E-01	2.40	4PD o
2s22p2 (3Pe)	1	3p	3	-6.91504E-01	2.40	4SPD o
2s22p2 (3Pe)	0	3p	5	-6.90584E-01	2.41	4PD o
2s22p2 (3Pe)	0	3p	7	-6.89268E-01	2.40	4D o
2s22p2 (3Pe)	1	3p	1	-6.76820E-01	2.43	4PD o
2s22p2 (3Pe)	0	3p	3	-6.76304E-01	2.43	4SPD o
2s22p2 (3Pe)	1	3p	5	-6.75356E-01	2.43	4PD o
2s22p2 (3Pe)	2	3p	3	-6.39512E-01	2.50	4SPD o
Nlv(c) = 8: set complete						
Nlv = 2, $^2L^e$: D (5 3)/2						
2s22p2 (1De)	2	3s	3	-6.70940E-01	2.44	2D e
2s22p2 (1De)	2	3s	5	-6.70932E-01	2.44	2D e
Nlv(c) = 2: set complete						
Eqv electron/unidentified levels, parity: e						
2s2p4			3	-5.81488E-01	0.00	2P e
2s2p4			1	-5.80052E-01	0.00	2P e
Nlv(c) = 2: set complete						
Nlv = 6, $^2L^o$: P (3 1)/2 D (5 3)/2 F (7 5)/2						
2s22p2 (1De)	2	3p	5	-4.69472E-01	2.52	2DF o
2s22p2 (1De)	2	3p	7	-4.69252E-01	2.42	2F o
2s22p2 (1De)	2	3p	5	-4.57328E-01	2.45	2DF o

(continued on next page)

Table 1 (continued)

$C_t(S_t L_t \pi_t)$		J_t	nl	$2J$	$E(\text{Ry})$	v	$SL\pi$
2s22p2	(1De)	2	3p	3	-4.57148E-01	2.46	2PD o
2s22p2	(1De)	2	3p	1	-4.34124E-01	2.53	2P o
2s22p2	(1De)	2	3p	3	-4.33704E-01	2.54	2PD o
Nlv(c) = 6: set complete							
Nlv = 11, $^4L^e$: P (5 3 1)/2 D (7 5 3 1)/2 F (9 7 5 3)/2							
2s22p2	(3Pe)	0	3d	3	-4.66992E-01	2.93	4PDF e
2s22p2	(3Pe)	1	3d	5	-4.66476E-01	2.92	4PDF e
2s22p2	(3Pe)	0	3d	7	-4.65724E-01	2.97	4DF e
2s22p2	(3Pe)	0	3d	9	-4.64728E-01	2.90	4F e
2s22p2	(3Pe)	1	3d	3	-4.54644E-01	2.96	4PDF e
2s22p2	(3Pe)	0	3d	5	-4.54576E-01	2.97	4PDF e
2s22p2	(3Pe)	0	3d	7	-4.53816E-01	2.97	4DF e
2s22p2	(3Pe)	2	3d	5	-4.51884E-01	2.97	4PDF e
2s22p2	(3Pe)	2	3d	3	-4.51312E-01	2.97	4PDF e
2s22p2	(3Pe)	2	3d	1	-4.51020E-01	2.97	4PD e
2s22p2	(3Pe)	2	3d	1	-4.45484E-01	2.99	4PD e
Nlv(c) = 11: set complete							
Nlv = 1, $^2L^e$: S (1)/2							
2s22p2	(1Se)	0	3s	1	-4.54648E-01	2.96	2S e
Nlv(c) = 1: set complete							
Nlv = 6, $^2L^e$: P (3 1)/2 D (5 3)/2 F (7 5)/2							
2s22p2	(3Pe)	1	3d	5	-4.52160E-01	2.97	2DF e
2s22p2	(3Pe)	1	3d	7	-4.50520E-01	2.98	2F e
2s22p2	(3Pe)	1	3d	3	-4.37716E-01	3.02	2PD e
2s22p2	(3Pe)	2	3d	1	-4.36456E-01	3.02	2P e
2s22p2	(3Pe)	2	3d	3	-4.35640E-01	3.02	2PD e
2s22p2	(3Pe)	2	3d	5	-4.35488E-01	3.02	2DF e
Nlv(c) = 6: set complete							
Nlv = 3, $^4L^e$: P (5 3 1)/2							
2s22p2	(3Pe)	0	4s	1	-4.04532E-01	3.14	4P e
2s22p2	(3Pe)	1	4s	3	-4.03636E-01	3.14	4P e
2s22p2	(3Pe)	2	4s	5	-4.02152E-01	3.14	4P e
Nlv(c) = 3: set complete							
Nlv = 2, $^2L^e$: P (3 1)/2							
2s22p2	(3Pe)	1	4s	1	-3.86597E-01	3.21	2P e
2s22p2	(3Pe)	2	4s	3	-3.85190E-01	3.21	2P e
Nlv(c) = 2: set complete							
Nlv = 1, $^6L^o$: S (5)/2							
2s22p2	(5So)	2	3s	5	-3.77695E-01	3.24	6S o
Nlv(c) = 1: set complete							
Nlv = 5, $^2L^o$: S (1)/2 P (3 1)/2 D (5 3)/2							
2s22p2	(3Pe)	2	4p	1	-3.45702E-01	3.39	2SP o
2s22p2	(3Pe)	1	4p	3	-3.16026E-01	3.55	2PD o
2s22p2	(3Pe)	2	4p	5	-3.14294E-01	3.55	2D o
2s22p2	(3Pe)	1	4p	1	-3.10326E-01	3.58	2SP o
2s22p2	(3Pe)	2	4p	3	-3.09523E-01	3.58	2PD o
Nlv(c) = 5: set complete							
Nlv = 8, $^4L^o$: S (3)/2 P (5 3 1)/2 D (7 5 3 1)/2							
2s22p2	(3Pe)	2	4p	3	-3.42561E-01	3.40	4SPD o
2s22p2	(3Pe)	0	4p	1	-3.38889E-01	3.44	4PD o
2s22p2	(3Pe)	1	4p	3	-3.38420E-01	3.43	4SPD o
2s22p2	(3Pe)	0	4p	5	-3.37580E-01	3.44	4PD o
2s22p2	(3Pe)	1	4p	7	-3.36272E-01	3.44	4D o
2s22p2	(3Pe)	1	4p	1	-3.33629E-01	3.46	4PD o
2s22p2	(3Pe)	2	4p	3	-3.33044E-01	3.45	4SPD o
2s22p2	(3Pe)	2	4p	5	-3.32233E-01	3.45	4PD o
Nlv(c) = 8: set complete							
Nlv = 9, $^2L^o$: S (1)/2 P (3 1)/2 D (5 3)/2 F (7 5)/2 G (9 7)/2							
2s22p2	(1De)	2	3d	5	-2.78404E-01	3.00	2DF e
2s22p2	(1De)	2	3d	7	-2.78350E-01	2.98	2FG e
2s22p2	(1De)	2	3d	7	-2.66414E-01	2.97	2FG e
2s22p2	(1De)	2	3d	9	-2.66410E-01	2.88	2G e
2s22p2	(1De)	2	3d	3	-2.61044E-01	2.91	2PD e
2s22p2	(1De)	2	3d	3	-2.58860E-01	3.00	2PD e
2s22p2	(1De)	2	3d	5	-2.58819E-01	2.90	2DF e
2s22p2	(1De)	2	3d	1	-2.56090E-01	2.94	2SP e
2s22p2	(1De)	2	3d	1	-2.36943E-01	3.08	2SP e

Table 1 (*continued*)

Table 2

E1 transition probabilities for observed levels of O II, grouped as fine structure components of LS multiplets. See page 870 for Explanation of Tables.

$C_i - C_k$	$T_i - T_k$	$g_i : l-g_j; K$	E_{ik} (Å)	f	S	A (s^{-1})
2s22p3–2s2p4	2Po–4Pe	2:1–2:1	1256.05	2.53E–07	2.09E–06	1.07E+03
2s22p3–2s2p4	2Po–4Pe	4:3–2:1	1256.05	2.83E–09	4.67E–08	2.39E+01
2s22p3–2s2p4	2Po–4Pe	2:1–4:1	1257.27	2.93E–09	2.43E–08	6.19E+00
2s22p3–2s2p4	2Po–4Pe	4:3–4:1	1257.27	6.00E–07	9.93E–06	2.53E+03
2s22p3–2s2p4	2Po–4Pe	4:3–6:1	1259.87	6.99E–07	1.16E–05	1.96E+03
2s2p4–2s22p2(3P)3p	4Pe–2So	2:1–2:2	1192.45	7.26E–07	5.70E–06	3.41E+03
2s2p4–2s22p2(3P)3p	4Pe–2So	4:1–2:2	1191.35	1.67E–06	2.62E–05	1.57E+04
2s2p4–2s22p2(3P)3p	4Pe–4Do	2:1–2:3	1154.07	1.10E–03	8.37E–03	5.51E+06
2s2p4–2s22p2(3P)3p	4Pe–4Do	2:1–4:4	1153.33	1.29E–03	9.80E–03	3.24E+06
2s2p4–2s22p2(3P)3p	4Pe–4Do	4:1–2:3	1153.05	7.58E–05	1.15E–03	7.60E+05
2s2p4–2s22p2(3P)3p	4Pe–4Do	4:1–4:4	1152.31	5.90E–04	8.95E–03	2.96E+06
2s2p4–2s22p2(3P)3p	4Pe–4Do	4:1–6:2	1151.08	1.54E–03	2.33E–02	5.17E+06
2s2p4–2s22p2(3P)3p	4Pe–4Do	6:1–4:4	1150.13	1.71E–05	3.88E–04	1.29E+05
2s2p4–2s22p2(3P)3p	4Pe–4Do	6:1–6:2	1148.91	2.36E–04	5.35E–03	1.19E+06
2s2p4–2s22p2(3P)3p	4Pe–4Do	6:1–8:1	1147.27	1.65E–03	3.74E–02	6.28E+06
LS	4Pe–4Do	12–20		2.09E–03	9.47E–02	6.31E+06
2s2p4–2s22p2(3P)3p	4Pe–4Po	2:1–2:4	1132.95	1.58E–03	1.18E–02	8.20E+06
2s2p4–2s22p2(3P)3p	4Pe–4Po	2:1–4:5	1132.35	7.67E–03	5.72E–02	2.00E+07
2s2p4–2s22p2(3P)3p	4Pe–4Po	4:1–2:4	1131.97	4.12E–03	6.14E–02	4.29E+07
2s2p4–2s22p2(3P)3p	4Pe–4Po	4:1–4:5	1131.36	1.28E–03	1.90E–02	6.66E+06
2s2p4–2s22p2(3P)3p	4Pe–4Po	4:1–6:3	1130.20	4.18E–03	6.22E–02	1.46E+07
2s2p4–2s22p2(3P)3p	4Pe–4Po	6:1–4:5	1129.26	3.13E–03	6.97E–02	2.45E+07
2s2p4–2s22p2(3P)3p	4Pe–4Po	6:1–6:3	1128.10	7.00E–03	1.56E–01	3.67E+07
LS	4Pe–4Po	12–12		9.80E–03	4.37E–01	5.12E+07
2s2p4–2s22p2(3P)3p	4Pe–2Po	2:1–2:5	1062.81	4.75E–08	3.32E–07	2.80E+02
2s2p4–2s22p2(3P)3p	4Pe–2Po	2:1–4:8	1062.14	5.91E–08	4.13E–07	1.75E+02
2s2p4–2s22p2(3P)3p	4Pe–2Po	4:1–2:5	1061.95	1.95E–07	2.72E–06	2.30E+03
2s2p4–2s22p2(3P)3p	4Pe–2Po	4:1–4:8	1061.28	1.38E–08	1.93E–07	8.17E+01
2s2p4–2s22p2(3P)3p	4Pe–2Po	6:1–4:8	1059.43	1.16E–06	2.42E–05	1.03E+04
2s2p4–2s22p2(1D)3p	4Pe–2Po	2:1–2:6	889.68	2.11E–09	1.23E–08	1.77E+01
2s2p4–2s22p2(1D)3p	4Pe–2Po	2:1–4:10	889.31	8.73E–07	5.11E–06	3.68E+03
2s2p4–2s22p2(1D)3p	4Pe–2Po	4:1–2:6	889.08	4.38E–08	5.13E–07	7.39E+02
2s2p4–2s22p2(1D)3p	4Pe–2Po	4:1–4:10	888.70	8.20E–07	9.60E–06	6.93E+03
2s2p4–2s22p2(1D)3p	4Pe–2Po	6:1–4:10	887.40	1.96E–07	3.44E–06	2.50E+03
2s2p4–2s22p2(3P)4p	4Pe–2So	2:1–2:7	800.28	9.75E–07	5.14E–06	1.02E+04
2s2p4–2s22p2(3P)4p	4Pe–2So	4:1–2:7	799.79	2.32E–06	2.45E–05	4.85E+04
2s2p4–2s22p2(3P)4p	4Pe–4Do	2:1–2:8	795.62	1.51E–05	7.92E–05	1.59E+05
2s2p4–2s22p2(3P)4p	4Pe–4Do	2:1–4:11	795.32	2.39E–02	1.25E–01	1.26E+08
2s2p4–2s22p2(3P)4p	4Pe–4Do	4:1–2:8	795.14	8.41E–07	8.81E–06	1.78E+04
2s2p4–2s22p2(3P)4p	4Pe–4Do	4:1–4:11	794.83	2.45E–02	2.57E–01	2.59E+08
2s2p4–2s22p2(3P)4p	4Pe–4Do	4:1–6:8	794.28	4.73E–05	4.95E–04	3.33E+05
2s2p4–2s22p2(3P)4p	4Pe–4Do	6:1–4:11	793.79	2.56E–02	4.02E–01	4.07E+08
2s2p4–2s22p2(3P)4p	4Pe–4Do	6:1–6:8	793.25	9.84E–06	1.54E–04	1.04E+05
2s2p4–2s22p2(3P)4p	4Pe–4Do	6:1–8:3	792.45	1.20E–05	1.88E–04	9.59E+04
LS	4Pe–4Do	12–20		2.50E–02	7.85E–01	1.58E+08
2s2p4–2s22p2(3P)4p	4Pe–4Po	2:1–2:9	792.14	2.55E–04	1.33E–03	2.72E+06
2s2p4–2s22p2(3P)4p	4Pe–4Po	2:1–4:13	791.12	2.66E–03	1.38E–02	1.42E+07
2s2p4–2s22p2(3P)4p	4Pe–4Po	4:1–2:9	791.66	6.59E–04	6.87E–03	1.40E+07
2s2p4–2s22p2(3P)4p	4Pe–4Po	4:1–4:13	790.64	9.39E–04	9.78E–03	1.00E+07
2s2p4–2s22p2(3P)4p	4Pe–4Po	4:1–6:9	790.82	6.74E–04	7.02E–03	4.79E+06
2s2p4–2s22p2(3P)4p	4Pe–4Po	6:1–4:13	789.61	3.22E–05	5.02E–04	5.16E+05
2s2p4–2s22p2(3P)4p	4Pe–4Po	6:1–6:9	789.79	1.11E–03	1.72E–02	1.18E+07
LS	4Pe–4Po	12–12		1.81E–03	5.65E–02	1.95E+07
2s2p4–2s22p2(3P)4p	4Pe–2Po	2:1–2:10	779.15	1.55E–08	7.94E–08	1.70E+02
2s2p4–2s22p2(3P)4p	4Pe–2Po	2:1–4:15	778.61	6.31E–06	3.23E–05	3.47E+04
2s2p4–2s22p2(3P)4p	4Pe–2Po	4:1–2:10	778.68	4.77E–08	4.89E–07	1.05E+03
2s2p4–2s22p2(3P)4p	4Pe–2Po	4:1–4:15	778.14	7.54E–06	7.73E–05	8.31E+04
2s2p4–2s22p2(3P)4p	4Pe–2Po	6:1–4:15	777.15	1.01E–05	1.55E–04	1.68E+05
2s2p4–2s22p2(1S)3p	4Pe–2Po	2:1–2:11	752.41	2.12E–10	1.05E–09	2.50E+00
2s2p4–2s22p2(1S)3p	4Pe–2Po	2:1–4:17	752.37	1.27E–08	6.27E–08	7.45E+01
2s2p4–2s22p2(1S)3p	4Pe–2Po	4:1–2:11	751.98	1.70E–08	1.68E–07	4.00E+02
2s2p4–2s22p2(1S)3p	4Pe–2Po	4:1–4:17	751.94	8.06E–10	7.99E–09	9.51E+00
2s2p4–2s22p2(1S)3p	4Pe–2Po	6:1–4:17	751.01	7.68E–08	1.14E–06	1.36E+03
2s2p4–2s22p2(3P)5p	4Pe–2So	2:1–2:13	711.21	1.75E–06	8.18E–06	2.30E+04
2s2p4–2s22p2(3P)5p	4Pe–2So	4:1–2:13	710.82	4.99E–06	4.67E–05	1.32E+05
2s2p4–2s22p2(3P)5p	4Pe–4Do	2:1–2:14	710.07	2.33E–09	1.09E–08	3.08E+01
2s2p4–2s22p2(3P)5p	4Pe–4Do	2:1–4:21	709.83	2.52E–05	1.18E–04	1.67E+05
2s2p4–2s22p2(3P)5p	4Pe–4Do	4:1–2:14	709.68	5.23E–06	4.88E–05	1.38E+05

Table 2 (continued)

$C_i - C_k$	$T_i - T_k$	$g_i : l-g_j : K$	E_{ik} (Å)	f	S	A (s^{-1})
$2s2p4-2s22p2(3P)5p$	$4Pe-4Do$	4:1-4:21	709.44	1.61E-05	1.50E-04	2.13E+05
$2s2p4-2s22p2(3P)5p$	$4Pe-4Do$	4:1-6:16	709.02	7.97E-06	7.44E-05	7.05E+04
$2s2p4-2s22p2(3P)5p$	$4Pe-4Do$	6:1-4:21	708.62	6.65E-06	9.30E-05	1.32E+05
$2s2p4-2s22p2(3P)5p$	$4Pe-4Do$	6:1-6:16	708.19	3.56E-05	4.98E-04	4.73E+05
$2s2p4-2s22p2(3P)5p$	$4Pe-4Do$	6:1-8:9	707.51	2.57E-06	3.60E-05	2.57E+04
LS	$4Pe-4Do$	12-20		3.64E-05	1.02E-03	2.90E+05
$2s2p4-2s22p2(3P)5p$	$4Pe-4Po$	2:1-2:15	708.55	9.57E-05	4.46E-04	1.27E+06
$2s2p4-2s22p2(3P)5p$	$4Pe-4Po$	2:1-4:22	708.31	6.37E-04	2.97E-03	4.23E+06
$2s2p4-2s22p2(3P)5p$	$4Pe-4Po$	4:1-2:15	708.16	2.30E-04	2.15E-03	6.12E+06
$2s2p4-2s22p2(3P)5p$	$4Pe-4Po$	4:1-4:22	707.93	1.44E-04	1.34E-03	1.92E+06
$2s2p4-2s22p2(3P)5p$	$4Pe-4Po$	4:1-6:17	707.45	2.53E-04	2.35E-03	2.24E+06
$2s2p4-2s22p2(3P)5p$	$4Pe-4Po$	6:1-4:22	707.10	7.88E-05	1.10E-03	1.58E+06
$2s2p4-2s22p2(3P)5p$	$4Pe-4Po$	6:1-6:17	706.63	3.69E-04	5.15E-03	4.93E+06
LS	$4Pe-4Po$	12-12		5.55E-04	1.55E-02	7.40E+06
$2s2p4-2s22p2(3P)5p$	$4Pe-2Po$	2:1-2:16	703.20	5.35E-08	2.48E-07	7.21E+02
$2s2p4-2s22p2(3P)5p$	$4Pe-2Po$	2:1-4:25	702.80	9.77E-04	4.52E-03	6.60E+06
$2s2p4-2s22p2(3P)5p$	$4Pe-2Po$	4:1-2:16	702.82	1.06E-07	9.82E-07	2.86E+03
$2s2p4-2s22p2(3P)5p$	$4Pe-2Po$	4:1-4:25	702.42	1.01E-03	9.37E-03	1.37E+07
$2s2p4-2s22p2(3P)5p$	$4Pe-2Po$	6:1-4:25	701.61	1.08E-03	1.49E-02	2.19E+07
$2s2p4-2s22p2(1D)4p$	$4Pe-2Po$	2:1-2:18	678.52	1.21E-06	5.42E-06	1.76E+04
$2s2p4-2s22p2(1D)4p$	$4Pe-2Po$	2:1-4:30	678.38	1.34E-05	6.00E-05	9.73E+04
$2s2p4-2s22p2(1D)4p$	$4Pe-2Po$	4:1-2:18	678.17	1.07E-05	9.53E-05	3.10E+05
$2s2p4-2s22p2(1D)4p$	$4Pe-2Po$	4:1-4:30	678.03	2.09E-05	1.87E-04	3.03E+05
$2s2p4-2s22p2(1D)4p$	$4Pe-2Po$	6:1-4:30	677.27	8.20E-06	1.10E-04	1.79E+05
$2s2p4-2s22p2(3P)6p$	$4Pe-2So$	2:1-2:19	674.36	3.28E-06	1.46E-05	4.81E+04
$2s2p4-2s22p2(3P)6p$	$4Pe-2So$	4:1-2:19	674.01	1.88E-06	1.67E-05	5.51E+04
$2s22p3-2s22p2(3P)3s$	$2Po-4Pe$	2:1-2:2	690.76	6.87E-07	3.12E-06	9.60E+03
$2s22p3-2s22p2(3P)3s$	$2Po-4Pe$	4:3-2:2	690.76	4.63E-06	4.21E-05	1.29E+05
$2s22p3-2s22p2(3P)3s$	$2Po-4Pe$	2:1-4:3	690.25	3.98E-06	1.81E-05	2.78E+04
$2s22p3-2s22p2(3P)3s$	$2Po-4Pe$	4:3-4:3	690.25	1.18E-05	1.07E-04	1.65E+05
$2s22p3-2s22p2(3P)3s$	$2Po-4Pe$	4:3-6:3	689.50	1.24E-07	1.12E-06	1.16E+03
$2s22p2(3P)3s-2s22p2(3P)3p$	$4Pe-2So$	2:2-2:2	5345.62	6.34E-05	2.23E-03	1.48E+04
$2s22p2(3P)3s-2s22p2(3P)3p$	$4Pe-2So$	4:3-2:2	5375.89	1.29E-04	9.10E-03	5.93E+04
$2s22p2(3P)3s-2s22p2(3P)3p$	$4Pe-4Do$	2:2-2:3	4652.17	2.26E-01	6.91E+00	6.96E+07
$2s22p2(3P)3s-2s22p2(3P)3p$	$4Pe-4Do$	2:2-4:4	4640.09	2.40E-01	7.33E+00	3.72E+07
$2s22p2(3P)3s-2s22p2(3P)3p$	$4Pe-4Do$	4:3-2:3	4675.08	1.99E-02	1.22E+00	1.21E+07
$2s22p2(3P)3s-2s22p2(3P)3p$	$4Pe-4Do$	4:3-4:4	4662.88	1.35E-01	8.31E+00	4.15E+07
$2s22p2(3P)3s-2s22p2(3P)3p$	$4Pe-4Do$	4:3-6:2	4642.93	2.96E-01	1.81E+01	6.10E+07
$2s22p2(3P)3s-2s22p2(3P)3p$	$4Pe-4Do$	6:3-4:4	4697.74	6.81E-03	6.32E-01	3.09E+06
$2s22p2(3P)3s-2s22p2(3P)3p$	$4Pe-4Do$	6:3-6:2	4677.48	6.84E-02	6.32E+00	2.09E+07
$2s22p2(3P)3s-2s22p2(3P)3p$	$4Pe-4Do$	6:3-8:1	4650.51	3.54E-01	3.25E+01	8.20E+07
LS	$4Pe-4Do$	12-20		4.43E-01	8.13E+01	8.19E+07
$2s22p2(3P)3s-2s22p2(3P)3p$	$4Pe-4Po$	2:2-2:4	4327.00	4.03E-02	1.15E+00	1.43E+07
$2s22p2(3P)3s-2s22p2(3P)3p$	$4Pe-4Po$	2:2-4:5	4318.19	2.14E-01	6.09E+00	3.83E+07
$2s22p2(3P)3s-2s22p2(3P)3p$	$4Pe-4Po$	4:3-2:4	4346.82	1.14E-01	6.53E+00	8.06E+07
$2s22p2(3P)3s-2s22p2(3P)3p$	$4Pe-4Po$	4:3-4:5	4337.92	4.57E-02	2.61E+00	1.62E+07
$2s22p2(3P)3s-2s22p2(3P)3p$	$4Pe-4Po$	4:3-6:3	4320.85	1.04E-01	5.93E+00	2.48E+07
$2s22p2(3P)3s-2s22p2(3P)3p$	$4Pe-4Po$	6:3-4:5	4368.07	7.76E-02	6.69E+00	4.07E+07
$2s22p2(3P)3s-2s22p2(3P)3p$	$4Pe-4Po$	6:3-6:3	4350.76	2.00E-01	1.72E+01	7.03E+07
LS	$4Pe-4Po$	12-12		2.69E-01	4.62E+01	9.50E+07
$2s22p2(3P)3s-2s22p2(3P)3p$	$4Pe-2Po$	2:2-2:5	3455.96	2.59E-06	5.89E-05	1.45E+03
$2s22p2(3P)3s-2s22p2(3P)3p$	$4Pe-2Po$	2:2-4:8	3448.90	3.47E-06	7.89E-05	9.74E+02
$2s22p2(3P)3s-2s22p2(3P)3p$	$4Pe-2Po$	4:3-2:5	3468.59	2.74E-06	1.25E-04	3.04E+03
$2s22p2(3P)3s-2s22p2(3P)3p$	$4Pe-2Po$	4:3-4:8	3461.47	8.39E-06	3.83E-04	4.67E+03
$2s22p2(3P)3s-2s22p2(3P)3p$	$4Pe-2Po$	6:3-4:8	3480.64	8.06E-07	5.54E-05	6.65E+02
$2s22p2(3P)3s-2s22p2(1D)3p$	$4Pe-2Po$	2:2-2:6	2116.62	2.62E-06	3.65E-05	3.90E+03
$2s22p2(3P)3s-2s22p2(1D)3p$	$4Pe-2Po$	2:2-4:10	2114.51	3.49E-07	4.86E-06	2.60E+02
$2s22p2(3P)3s-2s22p2(1D)3p$	$4Pe-2Po$	4:3-2:6	2121.35	1.74E-06	4.86E-05	5.15E+03
$2s22p2(3P)3s-2s22p2(1D)3p$	$4Pe-2Po$	4:3-4:10	2119.23	5.00E-06	1.39E-04	7.42E+03
$2s22p2(3P)3s-2s22p2(1D)3p$	$4Pe-2Po$	6:3-4:10	2126.40	5.57E-07	2.34E-05	1.23E+03
$2s22p2(3P)3s-2s22p2(3P)4p$	$4Pe-2So$	2:2-2:7	1672.17	1.49E-05	1.64E-04	3.55E+04
$2s22p2(3P)3s-2s22p2(3P)4p$	$4Pe-2So$	4:3-2:7	1675.12	2.31E-05	5.09E-04	1.10E+05
$2s22p2(3P)3s-2s22p2(3P)4p$	$4Pe-4Do$	2:2-2:8	1651.98	7.21E-03	7.84E-02	1.76E+07
$2s22p2(3P)3s-2s22p2(3P)4p$	$4Pe-4Do$	2:2-4:11	1650.67	1.97E-03	2.14E-02	2.41E+06
$2s22p2(3P)3s-2s22p2(3P)4p$	$4Pe-4Do$	4:3-2:8	1654.86	5.26E-04	1.15E-02	2.56E+06
$2s22p2(3P)3s-2s22p2(3P)4p$	$4Pe-4Do$	4:3-4:11	1653.54	1.47E-03	3.19E-02	3.58E+06
$2s22p2(3P)3s-2s22p2(3P)4p$	$4Pe-4Do$	4:3-6:8	1651.18	9.74E-03	2.12E-01	1.59E+07
$2s22p2(3P)3s-2s22p2(3P)4p$	$4Pe-4Do$	6:3-4:11	1657.90	1.11E-03	3.63E-02	4.03E+06

(continued on next page)

Table 2 (continued)

$C_i - C_k$	$T_i - T_k$	$g_i : l-g_j : K$	E_{ik} (Å)	f	S	A (s^{-1})
2s22p2(3P)3s–2s22p2(3P)4p	4Pe–4Do	6:3–6:8	1655.52	1.63E–03	5.32E–02	3.96E+06
2s22p2(3P)3s–2s22p2(3P)4p	4Pe–4Do	6:3–8:3	1652.07	1.08E–02	3.52E–01	1.98E+07
<i>LS</i>	4Pe–4Do	12–20		1.22E–02	7.97E–01	1.79E+07
2s22p2(3P)3s–2s22p2(3P)4p	4Pe–4Po	2:2–2:9	1637.06	5.61E–04	6.05E–03	1.40E+06
2s22p2(3P)3s–2s22p2(3P)4p	4Pe–4Po	2:2–4:13	1632.69	2.64E–03	2.84E–02	3.30E+06
2s22p2(3P)3s–2s22p2(3P)4p	4Pe–4Po	4:3–2:9	1639.88	2.34E–03	5.05E–02	1.16E+07
2s22p2(3P)3s–2s22p2(3P)4p	4Pe–4Po	4:3–4:13	1635.50	9.25E–04	1.99E–02	2.31E+06
2s22p2(3P)3s–2s22p2(3P)4p	4Pe–4Po	4:3–6:9	1636.26	1.21E–03	2.60E–02	2.00E+06
2s22p2(3P)3s–2s22p2(3P)4p	4Pe–4Po	6:3–4:13	1639.77	2.03E–03	6.57E–02	7.55E+06
2s22p2(3P)3s–2s22p2(3P)4p	4Pe–4Po	6:3–6:9	1640.53	4.45E–03	1.44E–01	1.10E+07
<i>LS</i>	4Pe–4Po	12–12		5.27E–03	3.41E–01	1.31E+07
2s22p2(3P)3s–2s22p2(3P)4p	4Pe–2Po	2:2–2:10	1582.50	1.21E–06	1.26E–05	3.23E+03
2s22p2(3P)3s–2s22p2(3P)4p	4Pe–2Po	2:2–4:15	1580.28	6.30E–07	6.56E–06	8.42E+02
2s22p2(3P)3s–2s22p2(3P)4p	4Pe–2Po	4:3–2:10	1585.14	7.11E–07	1.48E–05	3.77E+03
2s22p2(3P)3s–2s22p2(3P)4p	4Pe–2Po	4:3–4:15	1582.91	3.99E–06	8.31E–05	1.06E+04
2s22p2(3P)3s–2s22p2(3P)4p	4Pe–2Po	6:3–4:15	1586.91	1.83E–09	5.73E–08	7.27E+00
2s22p2(3P)3s–2s22p2(1S)3p	4Pe–2Po	2:2–2:11	1475.98	7.51E–07	7.30E–06	2.30E+03
2s22p2(3P)3s–2s22p2(1S)3p	4Pe–2Po	2:2–4:17	1475.83	6.62E–07	6.43E–06	1.01E+03
2s22p2(3P)3s–2s22p2(1S)3p	4Pe–2Po	4:3–2:11	1478.27	5.08E–07	9.89E–06	3.10E+03
2s22p2(3P)3s–2s22p2(1S)3p	4Pe–2Po	4:3–4:17	1478.13	2.44E–06	4.75E–05	7.44E+03
2s22p2(3P)3s–2s22p2(1S)3p	4Pe–2Po	6:3–4:17	1481.61	1.95E–09	5.70E–08	8.88E+00
2s22p2(3P)3s–2s22p2(3P)5p	4Pe–2So	2:2–2:13	1325.36	5.75E–05	5.02E–04	2.18E+05
2s22p2(3P)3s–2s22p2(3P)5p	4Pe–2So	4:3–2:13	1327.22	2.82E–05	4.93E–04	2.14E+05
2s22p2(3P)3s–2s22p2(3P)5p	4Pe–4Do	2:2–2:14	1321.40	3.81E–03	3.31E–02	1.45E+07
2s22p2(3P)3s–2s22p2(3P)5p	4Pe–4Do	2:2–4:21	1320.58	4.89E–03	4.26E–02	9.36E+06
2s22p2(3P)3s–2s22p2(3P)5p	4Pe–4Do	4:3–2:14	1323.25	2.07E–04	3.60E–03	1.57E+06
2s22p2(3P)3s–2s22p2(3P)5p	4Pe–4Do	4:3–4:21	1322.42	1.71E–03	2.98E–02	6.53E+06
2s22p2(3P)3s–2s22p2(3P)5p	4Pe–4Do	4:3–6:16	1320.94	5.51E–03	9.58E–02	1.40E+07
2s22p2(3P)3s–2s22p2(3P)5p	4Pe–4Do	6:3–4:21	1325.21	1.51E–05	3.95E–04	8.60E+04
2s22p2(3P)3s–2s22p2(3P)5p	4Pe–4Do	6:3–6:16	1323.73	4.98E–04	1.30E–02	1.90E+06
2s22p2(3P)3s–2s22p2(3P)5p	4Pe–4Do	6:3–8:9	1321.33	5.70E–03	1.49E–01	1.63E+07
<i>LS</i>	4Pe–4Do	12–20		7.03E–03	3.67E–01	1.61E+07
2s22p2(3P)3s–2s22p2(3P)5p	4Pe–4Po	2:2–2:15	1316.14	2.11E–04	1.83E–03	8.13E+05
2s22p2(3P)3s–2s22p2(3P)5p	4Pe–4Po	2:2–4:22	1315.34	1.15E–03	9.92E–03	2.21E+06
2s22p2(3P)3s–2s22p2(3P)5p	4Pe–4Po	4:3–2:15	1317.96	1.43E–03	2.48E–02	1.10E+07
2s22p2(3P)3s–2s22p2(3P)5p	4Pe–4Po	4:3–4:22	1317.16	9.44E–04	1.64E–02	3.63E+06
2s22p2(3P)3s–2s22p2(3P)5p	4Pe–4Po	4:3–6:17	1315.51	3.43E–04	5.95E–03	8.83E+05
2s22p2(3P)3s–2s22p2(3P)5p	4Pe–4Po	6:3–4:22	1319.93	1.11E–03	2.90E–02	6.39E+06
2s22p2(3P)3s–2s22p2(3P)5p	4Pe–4Po	6:3–6:17	1318.27	2.99E–03	7.78E–02	1.15E+07
<i>LS</i>	4Pe–4Po	12–12		3.18E–03	1.66E–01	1.22E+07
2s22p2(3P)3s–2s22p2(3P)5p	4Pe–2Po	2:2–2:16	1297.82	3.28E–06	2.80E–05	1.30E+04
2s22p2(3P)3s–2s22p2(3P)5p	4Pe–2Po	2:2–4:25	1296.46	7.14E–05	6.09E–04	1.42E+05
2s22p2(3P)3s–2s22p2(3P)5p	4Pe–2Po	4:3–2:16	1299.60	1.85E–06	3.17E–05	1.46E+04
2s22p2(3P)3s–2s22p2(3P)5p	4Pe–2Po	4:3–4:25	1298.23	3.16E–05	5.41E–04	1.25E+05
2s22p2(3P)3s–2s22p2(3P)5p	4Pe–2Po	6:3–4:25	1300.92	1.68E–05	4.32E–04	9.94E+04
2s22p2(3P)3s–2s22p2(1D)4p	4Pe–2Po	2:2–2:18	1216.17	4.00E–04	3.21E–03	1.81E+06
2s22p2(3P)3s–2s22p2(1D)4p	4Pe–2Po	2:2–4:30	1215.72	2.92E–03	2.34E–02	6.59E+06
2s22p2(3P)3s–2s22p2(1D)4p	4Pe–2Po	4:3–2:18	1217.73	1.32E–05	2.12E–04	1.19E+05
2s22p2(3P)3s–2s22p2(1D)4p	4Pe–2Po	4:3–4:30	1217.28	7.69E–04	1.23E–02	3.46E+06
2s22p2(3P)3s–2s22p2(1D)4p	4Pe–2Po	6:3–4:30	1219.64	2.81E–07	6.77E–06	1.89E+03
2s22p2(3P)3s–2s22p2(3P)6p	4Pe–2So	2:2–2:19	1202.87	1.78E–03	1.41E–02	8.19E+06
2s22p2(3P)3s–2s22p2(3P)6p	4Pe–2So	4:3–2:19	1204.39	1.39E–04	2.20E–03	1.27E+06
2s22p3–2s22p2(3P)3s	2Po–2Pe	2:1–2:3	673.75	3.05E–02	1.35E–01	4.48E+08
2s22p3–2s22p2(3P)3s	2Po–2Pe	4:3–2:3	673.75	7.44E–03	6.60E–02	2.19E+08
2s22p3–2s22p2(3P)3s	2Po–2Pe	2:1–4:4	672.94	1.59E–02	7.03E–02	1.17E+08
2s22p3–2s22p2(3P)3s	2Po–2Pe	4:3–4:4	672.94	3.93E–02	3.48E–01	5.79E+08
<i>LS</i>	2Po–2Pe	6–6		4.66E–02	6.19E–01	6.88E+08
2s22p2(3P)3s–2s22p2(3P)3p	2Pe–2So	2:3–2:2	6642.86	6.55E–02	2.87E+00	9.91E+06
2s22p2(3P)3s–2s22p2(3P)3p	2Pe–2So	4:4–2:2	6723.23	6.15E–02	5.44E+00	1.81E+07
<i>LS</i>	2Pe–2So	6–2		6.28E–02	8.31E+00	2.80E+07
2s22p2(3P)3s–2s22p2(3P)3p	2Pe–4Do	2:3–2:3	5604.69	4.46E–06	1.65E–04	9.48E+02
2s22p2(3P)3s–2s22p2(3P)3p	2Pe–4Do	2:3–4:4	5587.17	1.21E–05	4.45E–04	1.29E+03
2s22p2(3P)3s–2s22p2(3P)3p	2Pe–4Do	4:4–2:3	5661.80	1.77E–08	1.32E–06	7.37E+00
2s22p2(3P)3s–2s22p2(3P)3p	2Pe–4Do	4:4–4:4	5643.92	4.97E–06	3.69E–04	1.04E+03
2s22p2(3P)3s–2s22p2(3P)3p	2Pe–4Do	4:4–6:2	5614.71	2.17E–05	1.60E–03	3.06E+03
2s22p2(3P)3s–2s22p2(3P)3p	2Pe–4Po	2:3–2:4	5139.40	9.67E–05	3.27E–03	2.44E+04
2s22p2(3P)3s–2s22p2(3P)3p	2Pe–4Po	2:3–4:5	5126.97	3.92E–06	1.32E–04	4.98E+02
2s22p2(3P)3s–2s22p2(3P)3p	2Pe–4Po	4:4–2:4	5187.38	1.18E–04	8.04E–03	5.83E+04

Table 2 (continued)

$C_i - C_k$	$T_i - T_k$	$g_i : l-g_j : K$	E_{ik} (Å)	f	S	A (s^{-1})
2s22p2(3P)3s–2s22p2(3P)3p	2Pe–4Po	4:4–4:5	5174.71	7.66E–06	5.22E–04	1.91E+03
2s22p2(3P)3s–2s22p2(3P)3p	2Pe–4Po	4:4–6:3	5150.44	4.69E–05	3.18E–03	7.85E+03
2s22p2(3P)3s–2s22p2(3P)3p	2Pe–2Po	2:3–2:5	3955.32	2.03E–01	5.29E+00	8.67E+07
2s22p2(3P)3s–2s22p2(3P)3p	2Pe–2Po	2:3–4:8	3946.08	9.89E–02	2.57E+00	2.12E+07
2s22p2(3P)3s–2s22p2(3P)3p	2Pe–2Po	4:4–2:5	3983.68	5.29E–02	2.78E+00	4.45E+07
2s22p2(3P)3s–2s22p2(3P)3p	2Pe–2Po	4:4–4:8	3974.30	2.59E–01	1.36E+01	1.09E+08
LS	2Pe–2Po	6–6		3.09E–01	2.42E+01	1.30E+08